Published in final edited form as:
Inflamm Bowel Dis. 2011 June ; 17(6): 1359–1372. doi:10.1002/ibd.21478.

The NLRP3 inflammasome plays key role in the regulation of intestinal homeostasis

Simon A. Hirota, Ph.D.[*,‡], **Jeffrey Ng, M.Sc.**[*,¶], **Alan Lueng**[*,‡], **Maitham Khajah, Ph.D.**[*], **Ken Parhar, MD**[*], **Yan Li, M.Sc.**[*], **Victor Lam, B.Sc.**[*,‡], **Mireille S. Potentier**[*,‡], **Kelvin Ng**[*], **Misha Bawa, B.Sc.**[*], **Donna-Marie McCafferty, Ph.D.**[*], **Kevin P. Rioux, MD/Ph.D.**[*,‡], **Subrata Ghosh, MD**[*,‡], **Ramnik J. Xavier, MD**[‖], **Sean P. Colgan, Ph.D.**[#], **Jurg Tschopp, Ph.D.**[**], **Daniel Muruve, MD**[¶], **Justin A. MacDonald, Ph.D.**[*], and **Paul L. Beck, MD/Ph.D.**[*,‡]

[*] Gastrointestinal Research Group, University of Calgary, Calgary, AB, Canada. [‡] Inflammation Research Network, University of Calgary, Calgary, AB, Canada. [¶] Immunology Research Group, University of Calgary, Calgary, AB, Canada. [‖] Center for Computational and Integrative Biology, Massachusetts General Hospital, Harvard Medical School, Broad Institute of MIT, Boston, Massachusetts, USA. [#] Mucosal Inflammation Program, Division of Gastroenterology, University of Colorado Health Sciences Center, Denver, USA. [**] Biochemistry, University of Lausanne, Dorigny, Switzerland.

Abstract

Attenuated innate immune responses to the intestinal microbiota have been linked to the pathogenesis of Crohn's disease (CD). Recent genetic studies have revealed that hypofunctional mutations of NLRP3, a member of the NOD-like receptor (NLR) superfamily, are associated with an increased risk of developing CD. NLRP3 is a key component of the inflammasome, an intracellular danger sensor of the innate immune system. When activated, the inflammasome triggers caspase-1-dependent processing of inflammatory mediators, such as IL-1β and IL-18. In the current study we sought to assess the role of the NLRP3 inflammasome in the maintenance of intestinal homeostasis through its regulation of innate protective processes. To investigate this role, $Nlrp3^{-/-}$ and wild-type (WT) mice were assessed in the DSS- and TNBS-models of experimental colitis. $Nlrp3^{-/-}$ mice were found to be more susceptible to experimental colitis, an observation that was associated with reduced IL-1β reduced anti-inflammatory cytokine IL-10, and reduced protective growth factor TGF-β. Macrophages isolated from $Nlrp3^{-/-}$ mice failed to respond to bacterial muramyl dipeptide. Furthermore, Nlrp3-deficient neutrophils exhibited reduced chemotaxis and enhanced spontaneous apoptosis, but no change in oxidative burst. Lastly, $Nlrp3^{-/-}$ mice displayed altered colonic β-defensin expression, reduced colonic antimicrobial secretions and a unique intestinal microbiota. Our data confirm an essential role for the NLRP3 inflammasome in the regulation of intestinal homeostasis and provide biological insight into disease mechanisms associated with increased risk of CD in individuals with NLRP3 mutations.

Keywords

NLRP3; inflammasome; defensin; microbiota; neutrophil

Address correspondence to: Dr. Simon A. Hirota (simon.hirota@ucalgary.ca) Phone: 403-220-2218 Fax: 403-270-0995.

Disclosures: no conflicts of interest exist

Introduction

The inflammatory bowel diseases (IBD), ulcerative colitis (UC) and Crohn's disease (CD) are immunological disorders characterized by chronic and relapsing inflammation. Although the exact etiology of IBD has yet to be elucidated, the current paradigm suggests that the chronic mucosal inflammation is driven by aberrant interactions between the mucosal immune system and luminal antigens in genetically susceptible individuals (1). Genome-wide association (GWA) studies have revealed a number of candidate genes that are associated with an increased risk of developing IBD.

One of the best characterized IBD susceptibility genes is NOD2/CARD15. Mutations in NOD2, an intracellular receptor of the innate immune system belonging to the NLR (nucleotide binding domain leucine-rich-repeat gene-containing) family of proteins, are well established to be associated with an increased risk for the development of CD (1). Such mutations confer hyporesponsiveness to bacterial antigens, suggesting that the initiation of chronic inflammation may involve an inability of the innate immune system to respond appropriately to the presence of intracellular bacteria (2,3). Indeed, monocytes from CD patients with disease-associated NOD2 mutations produce less mature IL-1β in response to microbial muramyl dipeptide (MDP), a peptidoglycan component of gram-positive and gram-negative bacteria (4). Interestingly, this profound decrease in IL-1β secretion was associated with an induction of IL-1β mRNA suggesting an overlying defect in NOD2-mediated IL-1β processing. NOD2 mutations are also associated with alterations in the intestinal microbiota, an effect that has been linked to reduced antimicrobial secretions from the intestinal epithelium (5,6). These data highlight the importance of the innate immune system in the maintenance of intestinal homeostasis. The promotion of barrier function and the efficient elimination of invading bacteria are two key innate immune processes that are necessary in preventing chronic activation of the mucosal immune system, a hallmark of IBD.

Recently, the NLRP sub-family of the NLR family of proteins, distinguished from the other NLRs by an N-terminal pyrin domain, has been implicated in the pathogenesis of chronic inflammatory conditions (7,8). The best characterized member of the NLRP sub-family is NLRP3, a close relative of NOD2, which has been shown to trigger IL-1β and IL-18 processing and release in response to a variety of pathogen and endogenous danger signals including monosodium urate crystals (MSU), adenosine triphospate (ATP), silica and asbestos (9-11). Activation of NLRP3 leads to recruitment of the adaptor protein ASC and of pro-caspase-1 to form a multiprotein complex termed the inflammasome. Inflammasome activation triggers the caspase-1-dependent processing of inflammatory molecules pro-IL-1β and pro-IL-18, allowing for the secretion of the mature forms of these cytokines (12). Hyperfunctional mutations in NLRP3 confer increased IL-1β processing and are associated with diffuse inflammatory conditions collectively termed cryopryin-associated periodic syndromes (CAPS) (13). In contrast to the mutations in CAPS that enhance NLRP3-dependent IL-1β release, GWA studies have found that polymorphisms conferring a hypofunctional NLRP3 phenotype are associated with CD (14,15), a scenario reminiscent of the NOD2 paradigm. In these studies, monocytes isolated from patients who were homozygous for the risk allele displayed reduced IL-1β release in response to NLRP3 activation.

Recent studies assessing the role of the inflammasome in models of experimental intestinal inflammation have revealed that mice deficient in Nlrp3, ASC or caspase-1 exhibit enhanced susceptibility to dextran sulphate sodium (DSS) and 2,4,6-trinitrobenzenesulfonic acid (TNBS). Zaki *et al*. (2010) reported that $Nlrp3^{-/-}$ mice exhibited severe transmural inflammation following oral DSS treatment, a phenotype that was dependent on Nlrp3-

deficiency in non-bone-marrow-derived tissues (16). Dupaul-Chicoine *et al*. (2010) also found that loss of Nlrp3 resulted in more severe DSS colitis and again it appeared that this was dependent on non-bone marrow derived tissues (17). They also found that it appeared that the increase in colitis severity was due to the impaired IL-18 processing and that the phenotype could be partially reversed with exogenous IL-18 (17). Allen *et al*. (2010) also found that loss of Nlrp3 resulted in increased DSS-induced intestinal injury and inflammation but their chimeric studies found that the increased disease severity was dependent on the loss of Nlrp3 in bone-marrow-derived cells (18). In complete contrast to the aforementioned studies, Bauer *et al*. (2010) recently reported that the loss of Nlrp3 or caspase-1 was protective in the DSS model of colitis and that *in vivo* inhibition of caspase-1 attenuated DSS-induced inflammation (19).

Given the contrasting data published regarding the mechanism through which the inflammasome regulates intestinal homeostasis, we sought to explore other mechanisms through which NLRP3 may function in the gastrointestinal tract. Our data confirm that Nlrp3$^{-/-}$ mice are markedly more susceptible to experimental colitis compared to their WT counterparts, displaying decreased expression of TGF-β and IL-10, and possessing significant defects in macrophage and neutrophil function. In addition, Nlrp3$^{-/-}$ mice had altered colonic β-defensin expression, reduced crypt bactericidal capacity and marked changes in the intestinal microbiota. Our data clearly shows that the NLRP3 inflammasome plays a broad role in the innate intestinal immune response and maintenance of intestinal homeostasis.

Material and Methods

Animals

Wild-type (WT, C57Bl/6 background) and Nlrp3$^{-/-}$ (C57Bl/6 background) mice were generated from Nlrp3+/- mice (a gift from Dr. Jurg Tschopp, University of Lausanne, Dorigny, Switzerland) and used between 8-10 weeks of age. All experiments involving animals were approved by the Animal Care Committee, University of Calgary.

Induction and assessment of colitis

Colitis was induced by the addition of dextran sulphate sodium (DSS, 2.5% wt/vol, molecular weight, 40,000; ICN Biomedical, Aurora, OH) added to the drinking water as we have described previously (20,21). Animals were assessed daily and mean body weights were recorded. DSS consumption was equal between groups. Mice were sacrificed at day 7 of DSS exposure. Hematocrit values were assessed as an index of blood loss and serum was collected for assessment nitric oxide levels. The entire colon was removed, opened along the mesenteric border and fecal material removed. Segments of tissue were flash frozen for assessment of tissue cytokine levels and myeloperoxidase (MPO) levels, an indicator of colonic granulocyte infiltration. Additional segments were fixed in 10% neutral-buffered formalin, embedded in paraffin, sectioned, and stained with H&E in standard fashion. The severity of colitis was scored histologically using 2 different parameters on coded slides in a blinded fashion. An inflammation score was used: 0, no inflammation; 1, increased inflammatory cells noted above the muscularis mucosa only; 2, increased inflammatory cells involving the submucosa and above; 3, increased inflammatory cells involving the muscularis and/or serosa (20). The extent of ulceration was determined by measuring the amount of ulceration on each section as measured along the muscularis mucosa (expressed as percentage ulcerated mucosa) (20). Following our studies in the DSS model, we assessed whether the increased susceptibility observed in Nlrp3$^{-/-}$ mice, occurred in another murine model of colitis. The TNBS (2,4,6-trinitrobenzenesulfonic acid) model of colitis was used with some modifications on our initial description of this model (22). Mice were given a

rectal administration of 100 μL TNBS (Sigma-Aldrich Ltd. catalogue No. 92823, Ontario, Canada) (30 mg/mL) in 20% EtOH. A 5F infant feeding tube catheter with side ports (Mallinckrodt Inc., St. Louis, MO; catalogue No. 85771) was inserted 2.5 cm (measured from the midway point between the 2 catheter side ports) up the colon, and the 100 μL of solution was slowly administered over 30 seconds while pressure was applied to the rectal area to prevent leakage. The tube was slowly removed, and the rectal pressure was maintained for a further 30 seconds. All animals were killed 3 days following administration of TNBS/EtOH. The severity of colitis was assessed by monitoring changes in body weight and inflammation via assessment of colonic myeloperoxidase levels. Histological assessment was performed in a blinded fashion using the following criteria: Inflammation score: 0, normal; 1, increased inflammatory cells in lamina propria; 2, increased inflammatory cells in submucosa; 3, dense inflammatory cell mass; 4, transmural inflammation. Epithelial damage score: 0, nil; 1, patchy loss of epithelium; 2, widespread loss of epithelium; 3, complete absence of epithelium with loss of normal colonic architecture (20).

Tissue myeloperoxidase assay

MPO activity was determined following a published protocol (23). Briefly, tissue samples were weighed and suspended in 50 mmol/L potassium phosphate buffer (pH 6.0) containing 5 mg/ml hexadecyltrimethylammonium bromide (Sigma Chemical Co.) at a ratio of 50 mg tissue to 1 ml of buffer. Tissues were homogenized by a polytron tissue homogenizer for 15 seconds, and 1 ml was decanted into sterile Eppendorf tubes and centrifuged at 12,000 rpm for 15 minutes. Using a microtiter plate scanner, 200 μl of the reaction mixture (containing 16.7 mg of o-dianisidine (Sigma Chemical Co.), 90 ml of distilled H2O, 10 ml of potassium-phosphate buffer, and 50 μl of 1% H_2O_2) was added to each well containing 7 μl of sample in a standard 96-well plate and three absorbance readings at 30-second intervals at 450 nm were recorded. MPO activity was measured in units/mg tissue, where one unit of MPO was defined as the amount needed to degrade 1 μmol of H_2O_2 per minute at room temperature.

Assessment of tissue cytokine levels

Colonic segments stored at −80°C were placed in ice-cold lysis buffer (250 μl/25 mg tissue; 10 mM Tris pH 7.5, 1% NP-40, 150 mM NaCl, and protease inhibitor cocktail) and minced with dissection scissors. Tissues were then homogenized by a polytron tissue homogenizer for 15 seconds and 1 ml was decanted into sterile Eppendorf tubes and centrifuged at 12,000 rpm for 15 minutes. The supernatant was then filtered through an Ultrafree-MC centrifugal filter device (Millipore Corp.) with centrifugation at 12,000 for 5 minutes. The protein concentration of the filtrate was assessed using Biorad Protein Assay reagent (Biorad) and all samples were equalized for protein concentration by dilution with lysis buffer. Cytokine levels were assessed using a Luminex XMap bead-based cytokine array according to the manufacturer's instructions (Luminex Corp). Briefly, pre-labeled beads were mixed and added to each well. Samples were prepared in triplicate at two different total protein concentrations (10 and 35 mg total protein) and added to their respective wells. Samples were incubated with beads for 2 hours and then washed 3 times and incubated with secondary antibodies for 1 hour. Following incubation, wells were washed and then beads assessed in the Luminex 200 System. Mean fluorescence values were measured and cytokine concentrations calculated using the prepared standards.

Assessment of serum nitrates/nitrates

To assess NO_x production during DSS-induced colitis, nitrate and nitrite in the plasma of both WT and $Nlrp3^{-/-}$ mice were assayed as described previously (20). A modified Greiss reaction kit (Bioxytech NO-540; Oxis Research, Montreal, QC, Canada) was used per the manufacturer's guidelines. An aliquot of 160 μl of plasma was added to 640 μl of 1%

$ZnSO_4$ followed by the addition of 800 μl of 55 mM NaOH; samples were then vortexed and centrifuged at 10,000 *g* for 10 minutes. Supernatant (1,000 μl) was added to the assay buffer, incubated for 20 minutes at room temperature, recentrifuged at 10,000 *g* for 30 s, and then incubated with the final reaction solutions for 20 minutes at room temperature, and absorbance was then measured at 540 nm. The absorbance was plotted against standards and fit with linear regression, followed by calculation of NO_x according to the manufacturer's recommendations.

Isolation of mouse macrophages

Mouse peritoneal macrophages were obtained by injecting mice with a 4% thioglycollate (BD-Biosciences) PBS solution for 72 hours before harvesting macrophages through peritoneal lavage. Macrophages were plated in complete RPMI media overnight and stimulated with 10 ng/mL of ultra-pure LPS (Invivogen) for 30 minutes prior to treatment. Cells were treated with muramyl dipeptide (MDP, 10μg/mL, Invivogen), monosodium urate crystals (MSU, 50μg/mL, Sigma-Aldrich), aluminum adjuvant (Alum, 500μg/mL, Sigma-Aldrich) and ATP (5 mM, Sigma-Aldrich) for 6 hours. Following treatment, culture supernatants were harvested and inflammasome activation was detected through Western blot analysis of IL-1β (RD Systems) in culture supernatants.

Isolation of mouse bone marrow-derived neutrophils

Neutrophils were isolated from the bone marrow of WT and $Nlrp3^{-\backslash-}$ mice as described by Lieber *et al*. (2004) (24). Briefly, femurs and tibias of the mice were dissected, the marrow flushed with phosphate buffered saline (PBS, PH=7.4) then centrifuged at 1300 rpm for 6 minutes at 4 °C. The marrow was layered on a 3-step Percoll (Amersham Bioscience) gradient (72 %, 64 %, and 52 %), and centrifuged at 2600 rpm for 30 minutes at 4 °C. Neutrophils were taken from the layer between the 64 % and 72 % Percoll and washed once with PBS and suspended in RPMI culture media plus 20 % fetal bovine serum (FBS) (GIBCO) at a concentration of 1.0×10^7 cells/ml.

In vitro under-agarose gel assay for neutrophil chemotaxis

The under-agarose assay was performed as described in detail by Heit *et al*. (2002) (25). In brief, Falcon 35 mm × 10 mm culture dishes were filled with 3 ml of a 1.2 % agarose solution. Three wells were created in the gel 2.5 mm apart in a horizontal line. Neutrophil chemotaxis towards KC (R&D Systems; 1.25μM), LTB_4 (Calbiochem; 1μM), C5a (Calbiochem; 1μM), or WKYMVm; fMLP peptide (Phoenix Pharmaceuticals; 1μM) was determined by loading the center well with 10 μl of the chemoattractant and the outer wells with 10 μl of WT and $Nlrp3^{-\backslash-}$ neutrophils (1×10^7 cells/ml). Control conditions were performed in the same experiments by adding 10 μl of PBS in the center well instead of the chemoattractant. Once loaded, the gels were incubated for 4 hours in a 37°C/5% CO_2 incubator, which allowed sufficient time for neutrophils to migrate the entire distance between the wells. The results were recorded by using a video camera attached to a ZEISS Axiovert 135 microscope for subsequent analysis. Neutrophil chemotaxis was determined by subtracting the number of cells which migrated toward the source of chemoattractant minus the number of cells which migrated in the opposite direction and expressed as a percentage of the total number of cells that migrated in either direction.

Assessment of spontaneous neutrophil apoptosis

Freshly isolated bone-marrow derived neutrophils were resuspended in RPMI culture media plus 20% FBS and plated in Falcon 35 mm × 10 mm culture dishes at a density of 1×10^6 cell/mL (6 separate dishes per animal). Once seeded, cells were incubated for 12 hours in a 37°C/5% CO_2 incubator. Following the incubation period, cells were stained for flow

cytometry to assess viability (7-AAD) and early apoptosis (Annexin-V) using the PE Annexin V Apoptosis Detection Kit I as per the manufacturer's instructions (BD Pharmingen). The 6 dishes per animal were stained in the following manner: 1: cells only (negative control), 2: cells stained with 7-AAD alone, 3: cells stained with Annexin-V-PE, 4-6: cells stained with 7-ADD and Annexin-V-PE (26,27).

Assessment of neutrophil superoxide production

To assess the function of Nlrp3-deficient neutrophils we assessed superoxide generation by measuring the reduction of cytochrome c as described previously (28). Briefly, reactions were prepared with cytochrome c (200 μM) and bone-marrow-derived neutrophils (5×10^5 cells). In some assays, superoxide dismutase (SOD, 1500 U) was included to quench superoxide accumulation. The reaction was initiated by stimulation with PMA (8 μM) or fMLP (8 mM). The reaction mixtures were mixed and incubated at 37 °C for 25 min, followed by harvesting of supernatant by centrifugation at 900 × g for 20 min at 4 °C. Reduced cytochrome c in the cell free supernatant was measured at 550 nm on a double beam spectrophotometer.

Terminal Restriction Fragment Polymorphism (TRFLP) Analysis

Wild-type mice were derived from littermates of the $Nlrp3^{+/-}$ heterozygotes that were used to establish the $Nlrp3^{-/-}$ line. Both animal lines were continuously housed in the same animal care facility, on the same animal rack, and received the same food and water. All samples were taken from female mice at 8 weeks of age. Gentle handling of the mice evoked passage of fecal pellets, which were immediately collected and stored at −70°C. Total DNA was then extracted from 2-3 fecal pellets (20-30 mg) from each mouse using the QIAamp DNA Stool Mini Kit (Qiagen, Mississauga, ON, Canada). The process was modified to ensure uniform bacterial DNA extraction by the addition of a 2 minute mechanical bead (0.1 mm zirconia:silica) beating step (29). PCR was performed with primers 8f (5′-AGAGTTTGATCCTGGCTCAG-3′) labelled with 6-FAM and 926r (5′-CCGTCAATTCCTTTRAGTTT-3′) which target part of the bacterial 16S rRNA gene (30). Standard PCR conditions were used: 94 °C for 2 minutes, 25 cycles of 94 °C for 1 minute, 56 °C for 1 minute, 72 °C for 1 minute, and a final extension at 72 °C for 10 minutes. Three independent PCR amplifications were performed on each stool sample and the products were pooled and purified using the QIAquick PCR Purification Kit (Qiagen). For terminal restriction fragment length polymorphism analyses (TRFLP), five μL of each pooled, purified PCR product was digested overnight at 37 °C with 10 U of HpaII (Invitrogen, Burlington, ON, Canada) and again purified. Approximately 5 ng of digested sample was injected into an ABI 3730XL Genetic Analyzer (University of Calgary, Core DNA Services) and fragment analysis was performed using the GeneMapper software package (ABI Biosystems, Streetsville, ON, Canada) and LIZ1200 (ABI Biosystems) as a size standard. Binning was performed at 1 bp and only peaks with a minimum peak threshold of 50 fluorescence units were included.

RNA isolation and qPCR analysis

Mouse colonic sections were removed and placed directly in Trizol and flash-frozen. Total RNA was extracted from biopsies and isolated cells populations using the Trizol method according to the manufacturer's instructions (Invitrogen). To quantify changes in gene expression an ABI 7500 real-time PCR thermocycler was used to survey mRNA levels. All RNA samples were reversed transcribed to cDNA using the RT2 First-strand kit (SABiosciences). All primers were purchased from SABiosciences. PCR reactions were composed of primers, cDNA and RT2 real-time SYBR Green/Rox PCR master mix. Amplification plots were examined with the accompanying Sequence Detection Software to determine the threshold cycle (Ct). In all reactions endogenous control (GAPDH) was

amplified, and the Ct was determined. Data are expressed a fold-change calculated using the ΔΔCt method (31).

Colonic crypt killing assay

The antimicrobial capacity of colonic crypt secretions was performed as described previously (32), with minor modifications. Colonic crypts were isolated from the naïve WT and Nlrp3$^{-/-}$ mice, resuspended in iPIPES buffer (10 mM PIPES; pH 7.4 and 137 mM NaCl) and counted. For experiments, 1000 crypts were incubated in 40 μL of iPIPES buffer at 37 °C for 30 min. Following this period, 10 μL of a crypt-free isolate was added to 10^4 *E. coli* (DH5α) in 200 μL of LB broth and incubated for 37 °C for 60 min. The antimicrobial capacity of crypt-culture extracts was assessed by counting the overnight growth of WT and Nlrp3$^{-/-}$ crypt-treated *E. coli*, and expressed as a percentage of the growth observed in untreated *E. coli* cultures.

Statistical Analysis

Data are presented as the mean ± standard error of the mean (SEM). Parametric data were analyzed using a 1-way ANOVA followed by a Dunnett Multiple Comparisons post-test. Nonparametric data (scoring) were analyzed using a Kruskal–Wallis test (nonparametric ANOVA) followed by a Dunn Multiple Comparisons post-test. An associated probability (P value) of <0.05 was considered significant. All statistical analysis was performed with Graph Pad Instat and Prism 3.0 programs (GraphPad, San Diego, CA).

TRFLP data were tabulated and analyzed by principal component analysis using SIMCA-P (v11.5) multivariate statistics software (Umetrics, Umeå, Sweden) to identify intrinsic clusters within our dataset and the key bacterial phylotypes that determine such clustering. Orthogonal-projection to latent structure-discriminant analysis (O-PLS-DA) was carried on TRFLP binary data (*i.e.* peak presence or absence) using unit variance scaling. OPL-S coefficients were used to visualize the major variables contributing to the discrimination in the model. The model was subject to 7-fold cross validation, an iterative process whereby one-seventh of the samples were excluded and used to predict fit into the modified model. The Q^2 value represents how accurately the model predicts the dataset.

On this basis of OPL-S coefficients, several terminal restriction fragments (TRFs) were identified as the main factors driving the discriminant model. These TRFs were then used to identify major bacterial phylotypes that distinguished wild type and NLRP3 knock out mice. A virtual digest (ISPaR) with HpaII and primers 8f-926r of the HQ database (containing only mammalian gut bacterial 16S rRNA gene sequences) on the MiCA website (Microbial Community Analysis, version 3, Department of Biological Sciences, University of Idaho, http://mica.ibest.uidaho.edu/) was performed to generate a list of accession numbers for each terminal restriction fragment (TRF). This list was uploaded to SEQCART on the Ribosomal Database Project website (http://rdp.cme.msu.edu/) and a reference library was created (33). The TRFs of interest were compared to this reference library and a list of putative gut microbes comprising each profile was generated. Only TRFs that had 100% identity with predicted TRFs at the phylum level were matched to their respective accession numbers.

Results

Nlrp3$^{-/-}$ mice are more susceptible to experimental colitis

Throughout the course of DSS exposure, Nlrp3$^{-/-}$ mice exhibited significantly greater weight loss (Fig.1A) than their WT counterparts. Furthermore, Nlrp3$^{-/-}$ mice displayed significantly lower hematocrits, indicative of increased fecal blood loss (Fig.1B), higher MPO levels (Fig.1C) and more severe injury and inflammation upon histological assessment

(Fig.1D-E). As observed with DSS, Nlrp3$^{-/-}$ mice were more susceptible to TNBS as indicated by significantly greater weight loss (Fig.2A), elevated colonic MPO (Fig.2B), enhanced inflammation and tissue damage (Fig.2C-D).

The profiles of inflammatory mediators are altered in Nlrp3$^{-/-}$ mice exposed to DSS

The role NLRP3 inflammasome plays a key role in the processing of IL-1β. As expected, the Nlrp3$^{-/-}$ had lower levels of IL-1β during DSS colitis (Fig.3A). Increased NO_x was noted in the Nlrp3$^{-/-}$ mice (Fig.3B). Strikingly, at day-7 of DSS exposure, the Nlrp3$^{-/-}$ mice had significantly lower levels of the protective molecules IL-10 and TGF-β compared to WT (Fig.3C-D). Interestingly, Nlrp3$^{-/-}$ mice had decreased colonic tissue levels of the chemokines IP-10 and KC (Fig.3E-F). No significant changes were noted in MIP-1α and MIP-2 (see Supplementary Fig.1).

Nlrp3-deficient macrophages lack functional responses to bacterial muramyl dipeptide

Given that monocytes isolated from patients with CD-associated NOD2 mutations fail to respond to bacterial products (34,35), we sought to assess whether the loss of NLRP3 would alter the response to bacterial muramyl dipeptide, a potent NLR activator. Pretreatment of mouse peritoneal macrophages, both WT and Nlrp3$^{-/-}$ cells, with ultra-pure LPS triggers the production of pro-IL-1β through a TLR-4-dependent pathway (36). Subsequent exposure of WT macrophages to MDP triggered the processing and release of the mature IL-1β into the culture supernatant, which was abolished by glyburide, a purported selective inhibitor of the NLRP3-inflammasome(37) (Fig.4A). MDP-induced IL-1β processing and release was absent in macrophages isolated from Nlrp3$^{-/-}$ mice (Fig.4B). Standard inflammasome activators MSU, Alum and ATP induced IL-1β processing which was blocked by the NLRP3 inhibitor, glyburide, and was absent in Nlrp3$^{-/-}$ macrophages (Fig.4A-B).

Nlrp3-deficient neutrophils exhibit impaired chemotaxis and enhanced spontaneous apoptosis

Neutrophils play a key role in the innate immune response within the intestinal mucosa (38). Patients with Muckle-Wells syndrome (a multisystem inflammatory disease, due to a mutation of NLRP3) have defects in neutrophil chemotaxis (39). Using the under-agarose assay to assess neutrophil movement, it was revealed that bone-marrow-derived Nlrp3$^{-/-}$ neutrophils displayed significantly increased chemokinesis (i.e. non-directional chemokine induced movement) (Fig.5A), but significantly reduced chemotaxis towards KC, WKTMVm and C5a (Fig.5B). Altered caspase-1 signaling can also impact neutrophil survival (40). Consistent with this we found that bone-marrow-derived neutrophils isolated from Nlrp3$^{-/-}$ mice exhibited significantly greater levels of spontaneous apoptosis (Fig.5C). To further assess neutrophil function we measured superoxide production in response to PMA and fMLP stimulation. PMA-induced superoxide production was no different in Nlrp3-deficient neutrophils when compared to WT cells (Fig.5D). fMLP stimulated Nlrp3-deficient neutrophils produced similar overall superoxide levels, but exhibited reduced production at early time-points (Fig.5E).

Nlrp3-deficient mice exhibit altered colonic β-defensin expression and decreased antimicrobial capacity

NLR signaling has been linked to the regulation of Paneth cell function and the release of antimicrobial compounds terms defensins (5,41). Reduced defensin expression has been associated with CD patients expressing hypofunctional NOD2 mutations (5,41). Given the colonic nature of the injury observed in our model, we sought to assess the expression of select colonic β-defensins in Nlrp3$^{-/-}$ mice. Marked changes in β-defensin transcript expression were observed in both naïve and DSS-treated animals (Fig.6A-B). Naïve

Nlrp3$^{-/-}$ mice produced similar levels of *defb2*/MBD-2, *defb3*/MBD-3 and *defb4*/MBD-4, but markedly higher levels of *defb1*/MBD-1. At day-7 DSS, Nlrp3$^{-/-}$ mice had reduced expression of *defb1*/MBD-1 and *defb4*/MBD-4, but increased expression of *defb3*/MBD-3 compared to WT (Fig.6A-B). Alterations in defensin expression were associated with a reduction in the antimicrobial capacity of Nlrp3$^{-/-}$ crypt secretions when assessed in a bacterial killing assay (Fig.6C).

The intestinal microbiota is altered in Nlrp3$^{-/-}$ mice

Considerable attention has been paid to the role of the intestinal microbiota in the maintenance of intestinal homeostasis. Effective microbial clearance by the innate immune system and the release of protective antimicrobial secretions from the intestinal epithelium are thought to protect the mucosa from microbial insult and prevent inappropriate activation of the resident cells in the LP (1). Dysbiosis has been observed in IBD patients (42,43) and recently it has been shown that loss of NOD2 results in an altered intestinal microbiota in mice (44). Thus we sought to assess the microbiota in Nlrp3$^{-/-}$ mice. Although the WT mice used in these studies were derived from littermates of the Nlrp3$^{-/-}$ mice and continuously housed in the identical animal care facilities, their intestinal microbiota displayed marked differences. Supervised OPL-S discriminant analysis readily distinguished WT and Nlrp3$^{-/-}$ mice on the basis of fecal microbiota (Fig.6D). The Q^2 value of this model was excellent at 0.77; fecal TRFLP profiles were able to classify the two groups according to genotype with a reliable 77% accuracy. OPL-S coefficients revealed several TRFs that were significantly more common in WT animals and several TRFs that were significantly more common in Nlrp3$^{-/-}$ mice (Fig.6E). We were able to identify 6 bacterial genera in WT mice and 10 bacterial genera in Nlrp3$^{-/-}$ mice that differentiated these two lines at a 100% confidence level (Table 1). Of interest, in Nlrp3$^{-/-}$ mice, we detected potentially pathogenic members of *Enterobacteriaceae*, which at the genus level could match various species of *Citrobacter*, *Proteus* or *Shigella*. Also, the genus *Mycobacterium* was uniquely found in Nlrp3$^{-/-}$ mice, as were *Collinsella*, *Subdoligranulum*, *Clostridium and Ralstonia*.

Discussion

We confirm that Nlrp3-deficiency confers an enhanced susceptibility in two different experimental models of colitis. This NLRP3 paradigm appears reminiscent of the CD-related, hypofunctional mutations of NOD2 that have been found to impair responsiveness to microbial products and may regulate the intestinal microbiota (4,44,45). The parallels are even more intriguing since NOD2 and NLRP3 are members of the same NLR superfamily.

Activation of the NLRP3 inflammasome by danger- and/or pattern-associated molecular patterns results in caspase-1-dependent processing of the inflammatory cytokines IL-1β and IL-18 (12). Although hyperfunctional mutations of NLRP3 have been associated with several inflammatory conditions in humans, it is the hypofunctional mutations that are associated with an increased risk of CD. This is clearly supported by our data and others, which indicate that the loss of NLRP3 function results in an increased susceptibility to experimental colitis (16-18).

Interestingly, mice deficient in components of the innate immune system, including TLR family members and the downstream signaling molecule MyD88, also display enhanced susceptibility to chemically-induced colitis (46-49), suggesting that reduced microbial sensing may contribute to the initiation and perpetuation of intestinal inflammation. This is supported by observations that resistance to DSS- and TNBS-induced colitis can be conferred by strategies that enhance signaling through the innate immune system (i.e. MDP pretreatment) (50,51).

During assessment of the colonic cytokine/chemokine profiles following the 7-day DSS exposure, we observed striking differences between the WT and Nlrp3$^{-/-}$ mice. Nlrp3$^{-/-}$ mice exhibit a reduction in colonic IL-1β during intestinal inflammation. Furthermore, macrophages isolated from Nlrp3$^{-/-}$ mice failed to process and release IL-1β in response to MDP. Although these data appear paradoxical, given the pro-inflammatory role for IL-1β in many inflammatory conditions, the observation parallels the hyporesponsiveness and reduced IL-1β release observed in monocytes isolated from patients with Crohn's-associated NOD2 mutations (3,35).

The increased severity of colitis in the Nlrp3$^{-/-}$ mice was associated with higher levels of NOx and reduced expression of the anti-inflammatory cytokine IL-10 and the protective growth factor TGF-β. The associated higher levels of NOx in the Nlrp3$^{-/-}$ mice confirm previous work showing that NO plays a damaging or proinflammatory role in DSS colitis, an effect mediated by iNOS (20,52). The increased inflammation in the presence of decreased IL-10 and TGF-β was not unexpected given that previous studies have shown that targeted deletion of these protective mediators, or blockade of downstream signaling, leads an increased susceptibility to experimental colitis and the induction of spontaneous colitis (53,54). However, little is known about the NLRP3 inflammasome-dependent regulation of these cytokines.

Although the Nlrp3$^{-/-}$ mice had more severe colonic inflammation in response to DSS, there were reduced levels of the potent chemokines KC and IP-10, suggesting that these mediators are not essential for leukocyte recruitment and inflammation in DSS-induced colitis. The role of the inflammasome in the regulation of KC is controversial. Double-stranded RNA, a potent activator of the NLRP3 inflammasome (55), induces KC release in tissue macrophages (56) and airway tissue following *in vivo* challenge (57). However, Griffith *et al*. (2009) reported that hemozoin, a metabolite of hemoglobin and potent activator of the NLRP3 inflammasome, could induce inflammation and neutrophil migration when added to the peritoneal cavity but that MCP-1 and KC production was inflammasome independent (58).

Recent GWA studies have found that many of the genes associated with IBD encode components of the innate immune system (1), suggesting that IBD pathogenesis involves an impaired innate inflammatory response. In this paradigm, a delayed, or aberrant, inflammatory response to tissue injury or invasion of luminal bacteria fails to be effectively resolved and chronic inflammation is induced. There are several examples of innate immune defects resulting in intestinal inflammation, the most common being hypofunctional mutations of NOD2 in observed in CD patients. Defects resulting in decreased neutrophil numbers, such as congenital and cyclical neutropenia, and impaired neutrophil trafficking can result in a CD-like phenotype (38). Impaired leukocyte recruitment and phagocytic activity has also been described in CD (38). Marks *et al*. (2006) reported that CD patients displayed an aberrant innate immune response to tissue injury exhibiting reduced neutrophil accumulation and decreased expression of IL-8 and IL-1β 6 hours post-injury (59). Furthermore, CD patients inoculated with *E. coli* exhibited an attenuated inflammatory response (59). In keeping with the aforementioned reports, we found that neutrophils isolated from Nlrp3$^{-/-}$ mice have altered neutrophil migration and apoptosis. Nlrp3-deficient neutrophils exhibited attenuated chemotactic responses to KC, C5a and fMLP ligands and enhanced spontaneous apoptosis. However, there were no marked differences in neutrophil superoxide production in Nlrp3-deficient animals compared to WT mice. Further studies are required to fully assess the role of Nlrp3 in neutrophil function and how it impacts intestinal inflammation and homeostasis.

The intestinal epithelium plays a key role regulating the mucosal inflammatory status. It has been postulated that one of the functions of the innate immune system is to drive processes that contribute to the restitution of the intestinal epithelium following injury. Indeed, Zaki *et al*. (2010) reported that deletion of Nlrp3 and caspase-1 reduced the capacity of the intestinal epithelium to recover following DSS-induced injury (16). Another important function of the innate immune system within the intestinal mucosa is the regulation and release of antimicrobial factors such as defensins (60). Interestingly, the NOD2 mutations associated with CD confer impaired Paneth cell function and attenuated defensin release (5,61). NOD2 and NLRP3, both members of the NLR family of receptors, share common downstream signaling (i.e. caspase-1-dependent IL-1β processing); however, it is not known if the NLRP3 inflammasome regulates defensin expression. Zaki *et al*. (2010) reported that Nlrp3$^{-/-}$ mice exhibited and enhanced bacteremia following DSS-exposure (16). Furthermore, Dupaul-Chicoine *et al*. (2010) reported elevated levels of mucosally-associated bacteria in DSS-treated caspase-1-/- mice (17). Neither of these observations is surprising due to the markedly increased DSS-induced injury and inflammation in these animals compared to wild type mice. However, antibiotic treatment was able to normalize the Nlrp3$^{-/-}$ phenotype suggesting that the microbiota are integral in the driving the inflammation observed in these mice (16). Since other NLR's (e.g. NOD2) clearly regulate antimicrobial secretions, we hypothesized that the NLRP3 inflammasome may play a more direct role in regulating the antibacterial properties of the intestinal epithelium. To this end, we assessed the transcript levels for colonic defensins in Nlrp3-/- animals before and immediately following a 7-day course of DSS. The murine colon expresses β-defensins and, to date, 6 have been identified. Mouse β-defensins (MBD)-1 to -4 are the best characterized, and MBD-2 to -4 are highly inducible during bacterial infection or inflammatory responses (60). In human studies, the orthologue of MBD-3, human β-defensin 2, is significantly elevated in IBD patients, whereas human β-defensin 1 (MBD-1) is not changed (62). Our data reveal dysregulation of β-defensin expression in both naïve and DSS-exposed Nlrp3$^{-/-}$ mice compared to WT mice. Specifically, naïve Nlrp3$^{-/-}$ mice exhibited enhanced MBD-1 expression compared to WT mice, an effect which is lost upon DSS treatment. In addition to MBD-1, MBD-4 was also significantly reduced in Nlrp3$^{-/-}$ mice. MBD-2 expression was not different between naïve and DSS-treated Nlrp3$^{-/-}$ and WT mice, whereas MBD-3 was significantly elevated in response to DSS treatment. These observations parallel the upregulation of human β-defensin 2 in IBD patients during mucosal inflammation (62). Since both human and murine β-defensins are extremely difficult to assess at the protein level *in vivo* the above studies as well as our study assessed expression at the mRNA level. Despite this, we sought to define the general antimicrobial capacity of colonic crypt secretions using an established colonic crypt killing assay (32). Since Nlrp3-deficiency is associated with increased mucosal bacteria and systemic bacterial dissemination, we hypothesized that colonic crypts isolated from Nlrp3$^{-/-}$ mice would exhibit reduced bacterial killing capacity. Indeed colonic crypt secretions of Nlrp3$^{-/-}$ mice had significantly less antimicrobial activity when compared to WT mice. These data suggest that a loss in antimicrobial function, in conjunction with the previously reported failure to resolve following DSS-induced injury, may contribute to the elevated levels of mucosally-associated bacteria and the associated mucosal inflammation.

Intestinal dysbiosis has been linked to the etiology of IBD. Dupaul-Chicoine *et al*. (2010) reported that Nlrp3$^{-/-}$ mice exhibited greater bacterial loads within colonic isolates (17), however the composition of the microbiota was not assessed in this report. Thus we sought to profile the fecal microbiota from naïve Nlrp3$^{-/-}$ mice and their WT littermates. Remarkably, the fecal microbiota in Nlrp3$^{-/-}$ mice was dramatically different from that in WT mice which were bred from the same littermates and housed in the same facility, as was revealed by TRFLP analyses. Host genotype plays an essential role determining the composition of intestinal microbiota. For instance, loss of MyD88 alters Paneth cell

function, reducing defensin release and removing selective pressure that could allow remodelling of the microbiota (63). Similarly, a dysregulated β-defensin system in Nlrp3$^{-/-}$ mice may be a primary mediator of the dysbiosis observed in these mice. This is supported by the reduced antimicrobial capacity of secretions derived from crypts isolated from Nlrp3$^{-/-}$ mice compared to those isolated from WT mice. Interestingly, the observed microbial shifts were present in Nlrp3$^{-/-}$ mice prior to the induction of colitis, suggesting that bacterial dysbiosis may play a role in the increased susceptibility of these animals to experimental colitis. Dysbiosis has also been reported in mice deficient in another of the NLR family, NOD2 (44). This supports the theory that dysbiosis plays a predisposing role in the development of IBD in humans (64).

In summary, our studies indicate that loss of NLRP3 results in changes within several aspects of the innate immune system, and may directly influence the intestinal microbiota. Specifically, we confirm reports that Nlrp3$^{-/-}$ mice display enhanced susceptibly to experimental colitis (16-18). Moreover, our data also demonstrate alternative mechanisms that may explain the findings of the GWA studies showing that hypofunctional NRLP3 mutations are associated with Crohn's disease. We report that loss of NLRP3 was associated with; 1) reductions in the anti-inflammatory cytokine IL-10 and protective growth factor TGF-β expression during colitis, 2) underlying functional defects of Nlrp3-deficient macrophages and neutrophils, 3) dysregulation of β-defensin expression, 4) impaired crypt bactericidal activity and 5) dramatic alterations in intestinal microbiota. Many of these changes have also been observed in patients with IBD (62,65-69). These data suggest that a loss of NLRP3 function confers susceptibility for Crohn's disease by reducing the propensity of innate mechanisms to immediately combat mucosal insult by the intestinal microbiota, resulting in the induction of chronic inflammation. Furthermore, some of the changes noted in the Nlrp3-/- mice have been described with the hypofunction mutations of NOD2 that are associated with Crohn's disease. These studies further support the hypothesis that innate immune signaling by NLRs (including both NLRP3 and NOD2) play critical roles regulation of intestinal inflammation and maintenance of intestinal homeostasis.

Supplementary Material

Refer to Web version on PubMed Central for supplementary material.

Acknowledgments

The authors would like to thank Drs. Rustem Shaykhutdinov and Hans Vogel, University of Calgary, for their help in the analysis of the TFLRP data.

Funding: This work was supported by a CAG/CIHR and AHFMR fellowships (S.H.), CRC and AHFMR Senior Scholar award (J.A.M.), NIH grants DK50189, DE13499 and HL60569 (S.P.C.), a grant from the CCFA (S.P.C.) and AHFMR Clinical Investigator (P.L.B.).

Abbreviations

CD	Crohn's disease
UC	ulcerative colitis
DSS	dextran sulphate sodium
TNBS	2,4,6-trinitrobenzenesulfonic acid
WT	wild-type
NLR	nucleotide binding domain leucine-rich-repeat gene-containing

NLRP3	NLR family pyrin domain containing 3
GWA	genome wide association
MDP	muramyl dipeptide
MSU	monosodium urate
CAPS	cryopryin-associated periodic syndromes
BM	bone-marrow
NO_x	nitrate/nitrite
MPO	myeloperoxidase
H&E	hematoxylin and eosin
TRFLP	terminal restriction fragment polymorphism
OPL-S	Orthogonal-projection to latent structure
MBD	mouse β-defensin

References

1. Xavier RJ, Podolsky DK. Unravelling the pathogenesis of inflammatory bowel disease. Nature. 2007; 448:427–434. [PubMed: 17653185]
2. Hedl M, Li J, Cho JH, et al. Chronic stimulation of Nod2 mediates tolerance to bacterial products. Proc Natl Acad Sci U S A. 2007; 104:19440–19445. [PubMed: 18032608]
3. Netea MG, Ferwerda G, de Jong DJ, et al. NOD2 30-0insC mutation and the pathogenesis of Crohn's disease: impaired IL-1beta production points to a loss-of-function phenotype. Neth J Med. 2005; 63:305–308. [PubMed: 16186640]
4. Li J, Moran T, Swanson E, et al. Regulation of IL-8 and IL-1beta expression in Crohn's disease associated NOD2/CARD15 mutations. Hum Mol Genet. 2004; 13:1715–1725. [PubMed: 15198989]
5. Wehkamp J, Harder J, Weichenthal M, et al. NOD2 (CARD15) mutations in Crohn's disease are associated with diminished mucosal alpha-defensin expression. Gut. 2004; 53:1658–1664. [PubMed: 15479689]
6. Wehkamp J, Wang G, Kubler I, et al. The Paneth cell alpha-defensin deficiency of ileal Crohn's disease is linked to Wnt/Tcf-4. J Immunol. 2007; 179:3109–3118. [PubMed: 17709525]
7. Hoffman HM, Rosengren S, Boyle DL, et al. Prevention of cold-associated acute inflammation in familial cold autoinflammatory syndrome by interleukin-1 receptor antagonist. Lancet. 2004; 364:1779–1785. [PubMed: 15541451]
8. Jesus AA, Silva CA, Segundo GR, et al. Phenotype-genotype analysis of cryopyrin-associated periodic syndromes (CAPS): description of a rare non-exon 3 and a novel CIAS1 missense mutation. J Clin Immunol. 2008; 28:134–138. [PubMed: 18080732]
9. Dostert C, Petrilli V, Van Bruggen R, et al. Innate immune activation through Nalp3 inflammasome sensing of asbestos and silica. Science. 2008; 320:674–677. [PubMed: 18403674]
10. Hornung V, Bauernfeind F, Halle A, et al. Silica crystals and aluminum salts activate the NALP3 inflammasome through phagosomal destabilization. Nat Immunol. 2008; 9:847–856. [PubMed: 18604214]
11. Petrilli V, Papin S, Dostert C, et al. Activation of the NALP3 inflammasome is triggered by low intracellular potassium concentration. Cell Death Differ. 2007; 14:1583–1589. [PubMed: 17599094]
12. Petrilli V, Dostert C, Muruve DA, et al. The inflammasome: a danger sensing complex triggering innate immunity. Curr Opin Immunol. 2007; 19:615–622. [PubMed: 17977705]
13. Shinkai K, McCalmont TH, Leslie KS. Cryopyrin-associated periodic syndromes and autoinflammation. Clin Exp Dermatol. 2008; 33:1–9. [PubMed: 17927785]

14. Villani AC, Lemire M, Fortin G, et al. Common variants in the NLRP3 region contribute to Crohn's disease susceptibility. Nat Genet. 2009; 41:71–76. [PubMed: 19098911]
15. Schoultz I, Verma D, Halfvarsson J, et al. Combined Polymorphisms in Genes Encoding the Inflammasome Components NALP3 and CARD8 Confer Susceptibility to Crohn's Disease in Swedish Men. Am J Gastroenterol. 2009
16. Zaki MH, Boyd KL, Vogel P, et al. The NLRP3 inflammasome protects against loss of epithelial integrity and mortality during experimental colitis. Immunity. 32:379–391. [PubMed: 20303296]
17. Dupaul-Chicoine J, Yeretssian G, Doiron K, et al. Control of intestinal homeostasis, colitis, and colitis-associated colorectal cancer by the inflammatory caspases. Immunity. 32:367–378. [PubMed: 20226691]
18. Allen IC, TeKippe EM, Woodford RM, et al. The NLRP3 inflammasome functions as a negative regulator of tumorigenesis during colitis-associated cancer. J Exp Med. 207:1045–1056. [PubMed: 20385749]
19. Bauer C, Duewell P, Mayer C, et al. Colitis induced in mice with dextran sulfate sodium (DSS) is mediated by the NLRP3 inflammasome. Gut.
20. Beck PL, Li Y, Wong J, et al. Inducible nitric oxide synthase from bone marrow-derived cells plays a critical role in regulating colonic inflammation. Gastroenterology. 2007; 132:1778–1790. [PubMed: 17449036]
21. Beck PL, Xavier R, Wong J, et al. Paradoxical roles of different nitric oxide synthase isoforms in colonic injury. Am J Physiol Gastrointest Liver Physiol. 2004; 286:G137–147. [PubMed: 14665440]
22. Morris GP, Beck PL, Herridge MS, et al. Hapten-induced model of chronic inflammation and ulceration in the rat colon. Gastroenterology. 1989; 96:795–803. [PubMed: 2914642]
23. Diaz-Granados N, Howe K, Lu J, et al. Dextran sulfate sodium-induced colonic histopathology, but not altered epithelial ion transport, is reduced by inhibition of phosphodiesterase activity. Am J Pathol. 2000; 156:2169–2177. [PubMed: 10854237]
24. Lieber JG, Webb S, Suratt BT, et al. The in vitro production and characterization of neutrophils from embryonic stem cells. Blood. 2004; 103:852–859. [PubMed: 14525782]
25. Heit B, Tavener S, Raharjo E, et al. An intracellular signaling hierarchy determines direction of migration in opposing chemotactic gradients. J Cell Biol. 2002; 159:91–102. [PubMed: 12370241]
26. Duffy AJ, Nolan B, Sheth K, et al. Inhibition of alveolar neutrophil immigration in endotoxemia is macrophage inflammatory protein 2 independent. J Surg Res. 2000; 90:51–57. [PubMed: 10781375]
27. Hodge GL, Flower R, Han P. Optimal storage conditions for preserving granulocyte viability as monitored by Annexin V binding in whole blood. J Immunol Methods. 1999; 225:27–38. [PubMed: 10365779]
28. Weening RS, Wever R, Roos D. Quantitative aspects of the production of superoxide radicals by phagocytizing human granulocytes. J Lab Clin Med. 1975; 85:245–252. [PubMed: 163283]
29. Zoetendal EG, Ben-Amor K, Akkermans AD, et al. DNA isolation protocols affect the detection limit of PCR approaches of bacteria in samples from the human gastrointestinal tract. Syst Appl Microbiol. 2001; 24:405–410. [PubMed: 11822677]
30. Liu WT, Marsh TL, Cheng H, et al. Characterization of microbial diversity by determining terminal restriction fragment length polymorphisms of genes encoding 16S rRNA. Appl Environ Microbiol. 1997; 63:4516–4522. [PubMed: 9361437]
31. Livak KJ, Schmittgen TD. Analysis of relative gene expression data using real-time quantitative PCR and the 2(-Delta Delta C(T)) Method. Methods. 2001; 25:402–408. [PubMed: 11846609]
32. Ayabe T, Satchell DP, Wilson CL, et al. Secretion of microbicidal alpha-defensins by intestinal Paneth cells in response to bacteria. Nat Immunol. 2000; 1:113–118. [PubMed: 11248802]
33. Wang Q, Garrity GM, Tiedje JM, et al. Naive Bayesian classifier for rapid assignment of rRNA sequences into the new bacterial taxonomy. Appl Environ Microbiol. 2007; 73:5261–5267. [PubMed: 17586664]
34. van Heel DA, Ghosh S, Butler M, et al. Muramyl dipeptide and toll-like receptor sensitivity in NOD2-associated Crohn's disease. Lancet. 2005; 365:1794–1796. [PubMed: 15910952]

35. van Heel DA, Hunt KA, King K, et al. Detection of muramyl dipeptide-sensing pathway defects in patients with Crohn's disease. Inflamm Bowel Dis. 2006; 12:598–605. [PubMed: 16804397]
36. Becker CE, O'Neill LA. Inflammasomes in inflammatory disorders: the role of TLRs and their interactions with NLRs. Semin Immunopathol. 2007; 29:239–248. [PubMed: 17805544]
37. Lamkanfi M, Mueller JL, Vitari AC, et al. Glyburide inhibits the Cryopyrin/Nalp3 inflammasome. J Cell Biol. 2009; 187:61–70. [PubMed: 19805629]
38. Rahman FZ, Marks DJ, Hayee BH, et al. Phagocyte dysfunction and inflammatory bowel disease. Inflamm Bowel Dis. 2008; 14:1443–1452. [PubMed: 18421761]
39. Lokuta MA, Cooper KM, Aksentijevich I, et al. Neutrophil chemotaxis in a patient with neonatal-onset multisystem inflammatory disease and Muckle-Wells syndrome. Ann Allergy Asthma Immunol. 2005; 95:394–399. [PubMed: 16279571]
40. Rowe SJ, Allen L, Ridger VC, et al. Caspase-1-deficient mice have delayed neutrophil apoptosis and a prolonged inflammatory response to lipopolysaccharide-induced acute lung injury. J Immunol. 2002; 169:6401–6407. [PubMed: 12444148]
41. Simms LA, Doecke JD, Walsh MD, et al. Reduced alpha-defensin expression is associated with inflammation and not NOD2 mutation status in ileal Crohn's disease. Gut. 2008; 57:903–910. [PubMed: 18305068]
42. Willing B, Halfvarson J, Dicksved J, et al. Twin studies reveal specific imbalances in the mucosa-associated microbiota of patients with ileal Crohn's disease. Inflamm Bowel Dis. 2009; 15:653–660. [PubMed: 19023901]
43. Prindiville T, Cantrell M, Wilson KH. Ribosomal DNA sequence analysis of mucosa-associated bacteria in Crohn's disease. Inflamm Bowel Dis. 2004; 10:824–833. [PubMed: 15626901]
44. Petnicki-Ocwieja T, Hrncir T, Liu YJ, et al. Nod2 is required for the regulation of commensal microbiota in the intestine. Proc Natl Acad Sci U S A. 2009; 106:15813–15818. [PubMed: 19805227]
45. Beynon V, Cotofana S, Brand S, et al. NOD2/CARD15 genotype influences MDP-induced cytokine release and basal IL-12p40 levels in primary isolated peripheral blood monocytes. Inflamm Bowel Dis. 2008; 14:1033–1040. [PubMed: 18383179]
46. Podolsky DK, Gerken G, Eyking A, et al. Colitis-associated variant of TLR2 causes impaired mucosal repair because of TFF3 deficiency. Gastroenterology. 2009; 137:209–220. [PubMed: 19303021]
47. Vijay-Kumar M, Wu H, Aitken J, et al. Activation of toll-like receptor 3 protects against DSS-induced acute colitis. Inflamm Bowel Dis. 2007; 13:856–864. [PubMed: 17393379]
48. Fukata M, Michelsen KS, Eri R, et al. Toll-like receptor-4 is required for intestinal response to epithelial injury and limiting bacterial translocation in a murine model of acute colitis. Am J Physiol Gastrointest Liver Physiol. 2005; 288:G1055–1065. [PubMed: 15826931]
49. Fukata M, Breglio K, Chen A, et al. The myeloid differentiation factor 88 (MyD88) is required for CD4+ T cell effector function in a murine model of inflammatory bowel disease. J Immunol. 2008; 180:1886–1894. [PubMed: 18209086]
50. Watanabe T, Asano N, Murray PJ, et al. Muramyl dipeptide activation of nucleotide-binding oligomerization domain 2 protects mice from experimental colitis. J Clin Invest. 2008; 118:545–559. [PubMed: 18188453]
51. Cario E, Gerken G, Podolsky DK. Toll-like receptor 2 controls mucosal inflammation by regulating epithelial barrier function. Gastroenterology. 2007; 132:1359–1374. [PubMed: 17408640]
52. Hokari R, Kato S, Matsuzaki K, et al. Reduced sensitivity of inducible nitric oxide synthase-deficient mice to chronic colitis. Free Radic Biol Med. 2001; 31:153–163. [PubMed: 11440827]
53. Sakuraba H, Ishiguro Y, Yamagata K, et al. Blockade of TGF-beta accelerates mucosal destruction through epithelial cell apoptosis. Biochem Biophys Res Commun. 2007; 359:406–412. [PubMed: 17560553]
54. de Vries JE. Immunosuppressive and anti-inflammatory properties of interleukin 10. Ann Med. 1995; 27:537–541. [PubMed: 8541028]
55. Kanneganti TD, Ozoren N, Body-Malapel M, et al. Bacterial RNA and small antiviral compounds activate caspase-1 through cryopyrin/Nalp3. Nature. 2006; 440:233–236. [PubMed: 16407888]

56. De Filippo K, Henderson RB, Laschinger M, et al. Neutrophil chemokines KC and macrophage-inflammatory protein-2 are newly synthesized by tissue macrophages using distinct TLR signaling pathways. J Immunol. 2008; 180:4308–4315. [PubMed: 18322244]
57. Londhe VA, Belperio JA, Keane MP, et al. CXCR2 is critical for dsRNA-induced lung injury: relevance to viral lung infection. J Inflamm (Lond). 2005; 2:4. [PubMed: 15921526]
58. Griffith JW, Sun T, McIntosh MT, et al. Pure Hemozoin is inflammatory in vivo and activates the NALP3 inflammasome via release of uric acid. J Immunol. 2009; 183:5208–5220. [PubMed: 19783673]
59. Marks DJ, Harbord MW, MacAllister R, et al. Defective acute inflammation in Crohn's disease: a clinical investigation. Lancet. 2006; 367:668–678. [PubMed: 16503465]
60. Wehkamp J, Schauber J, Stange EF. Defensins and cathelicidins in gastrointestinal infections. Curr Opin Gastroenterol. 2007; 23:32–38. [PubMed: 17133082]
61. Bevins CL, Stange EF, Wehkamp J. Decreased Paneth cell defensin expression in ileal Crohn's disease is independent of inflammation, but linked to the NOD2 1007fs genotype. Gut. 2009; 58:882–883. discussion 883-884. [PubMed: 19433600]
62. Wehkamp J, Fellermann K, Herrlinger KR, et al. Human beta-defensin 2 but not beta-defensin 1 is expressed preferentially in colonic mucosa of inflammatory bowel disease. Eur J Gastroenterol Hepatol. 2002; 14:745–752. [PubMed: 12169983]
63. Vaishnava S, Behrendt CL, Ismail AS, et al. Paneth cells directly sense gut commensals and maintain homeostasis at the intestinal host-microbial interface. Proc Natl Acad Sci U S A. 2008; 105:20858–20863. [PubMed: 19075245]
64. Tamboli CP, Neut C, Desreumaux P, et al. Dysbiosis in inflammatory bowel disease. Gut. 2004; 53:1–4. [PubMed: 14684564]
65. Aldhous MC, Noble CL, Satsangi J. Dysregulation of human beta-defensin-2 protein in inflammatory bowel disease. PLoS One. 2009; 4:e6285. [PubMed: 19617917]
66. Kapel N, Benahmed N, Morali A, et al. Fecal beta-defensin-2 in children with inflammatory bowel diseases. J Pediatr Gastroenterol Nutr. 2009; 48:117–120. [PubMed: 19172136]
67. Witthoft T, Pilz CS, Fellermann K, et al. Enhanced human beta-defensin-2 (hBD-2) expression by corticosteroids is independent of NF-kappaB in colonic epithelial cells (CaCo2). Dig Dis Sci. 2005; 50:1252–1259. [PubMed: 16047468]
68. Fahlgren A, Hammarstrom S, Danielsson A, et al. beta-Defensin-3 and -4 in intestinal epithelial cells display increased mRNA expression in ulcerative colitis. Clin Exp Immunol. 2004; 137:379–385. [PubMed: 15270856]
69. Wehkamp J, Harder J, Weichenthal M, et al. Inducible and constitutive beta-defensins are differentially expressed in Crohn's disease and ulcerative colitis. Inflamm Bowel Dis. 2003; 9:215–223. [PubMed: 12902844]

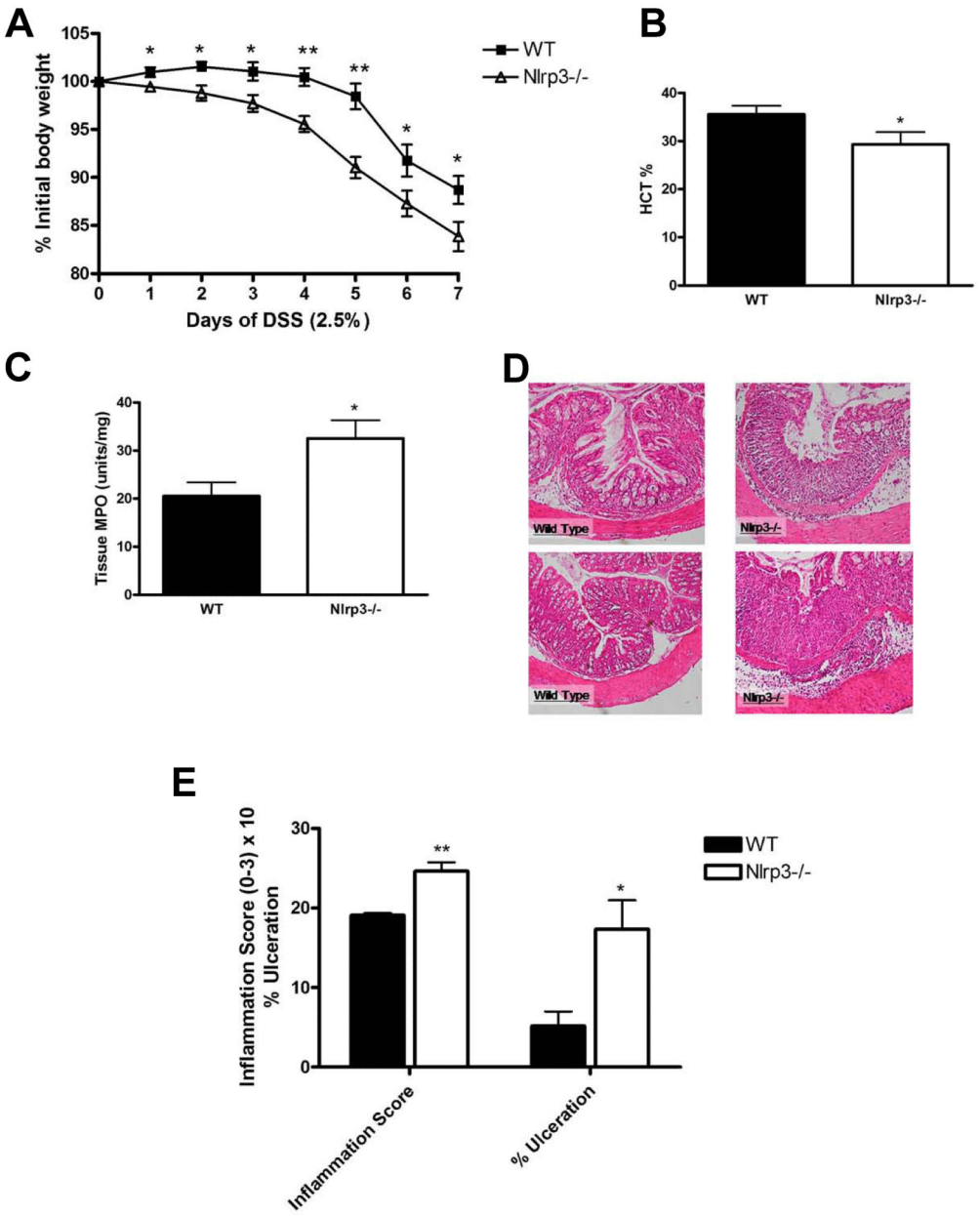

Figure 1.

Nlrp3$^{-/-}$ mice exhibit enhanced susceptibility to DSS-induced colitis as exhibited by accelerated weight loss (A); reduced hematocrit (B); increased colonic MPO (C). Nlrp3$^{-/-}$ mice exposed to DSS exhibited significantly more inflammation, elevated damage score and overall magnitude of ulceration (D-E; Inflammation score ×10), which is evident in colonic sections stained with H&E. N=8-12; * denotes $p<0.05$ compared to WT mice; ** denotes $p<0.005$ compared to WT mice.

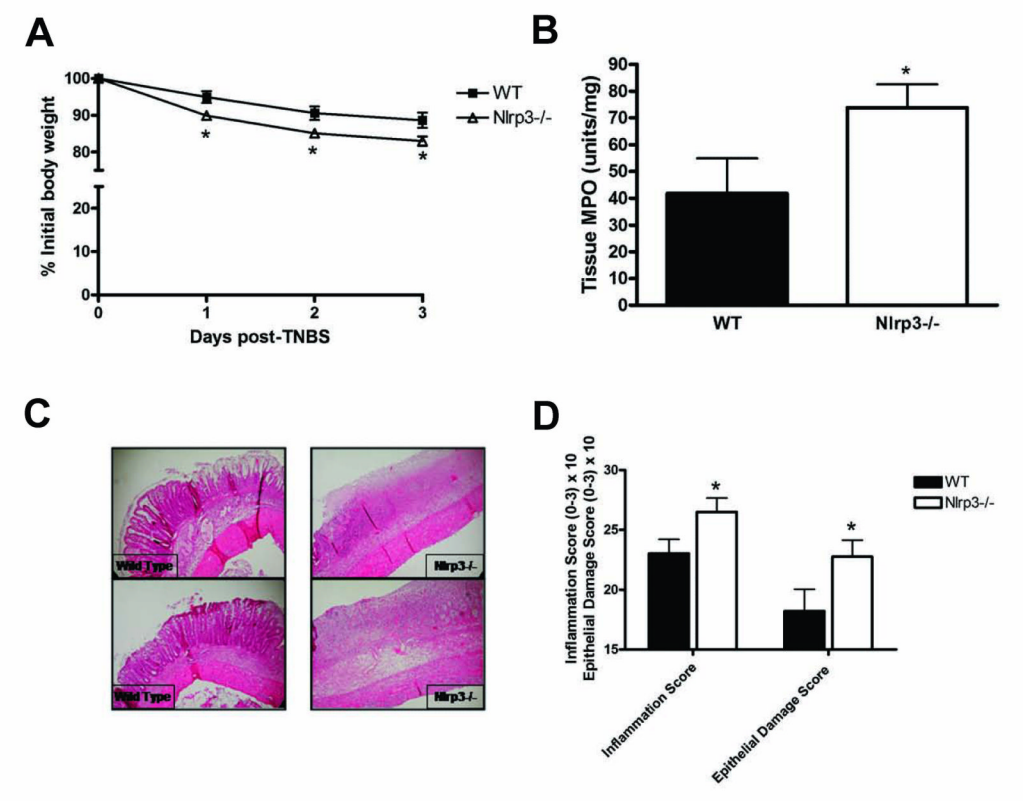

Figure 2.

Nlrp3$^{-/-}$ mice exhibit enhanced susceptibility to TNBS-induced colitis as exhibited by accelerated weight loss (A) and increased colonic MPO (B). Nlrp3$^{-/-}$ mice exposed to TNBS exhibited significantly more inflammation and elevated damage which is evident in colonic sections stained with H&E (C) and quantified by blinded histological assessment (D). N=8/group; * denotes $p<0.05$ compared to WT mice.

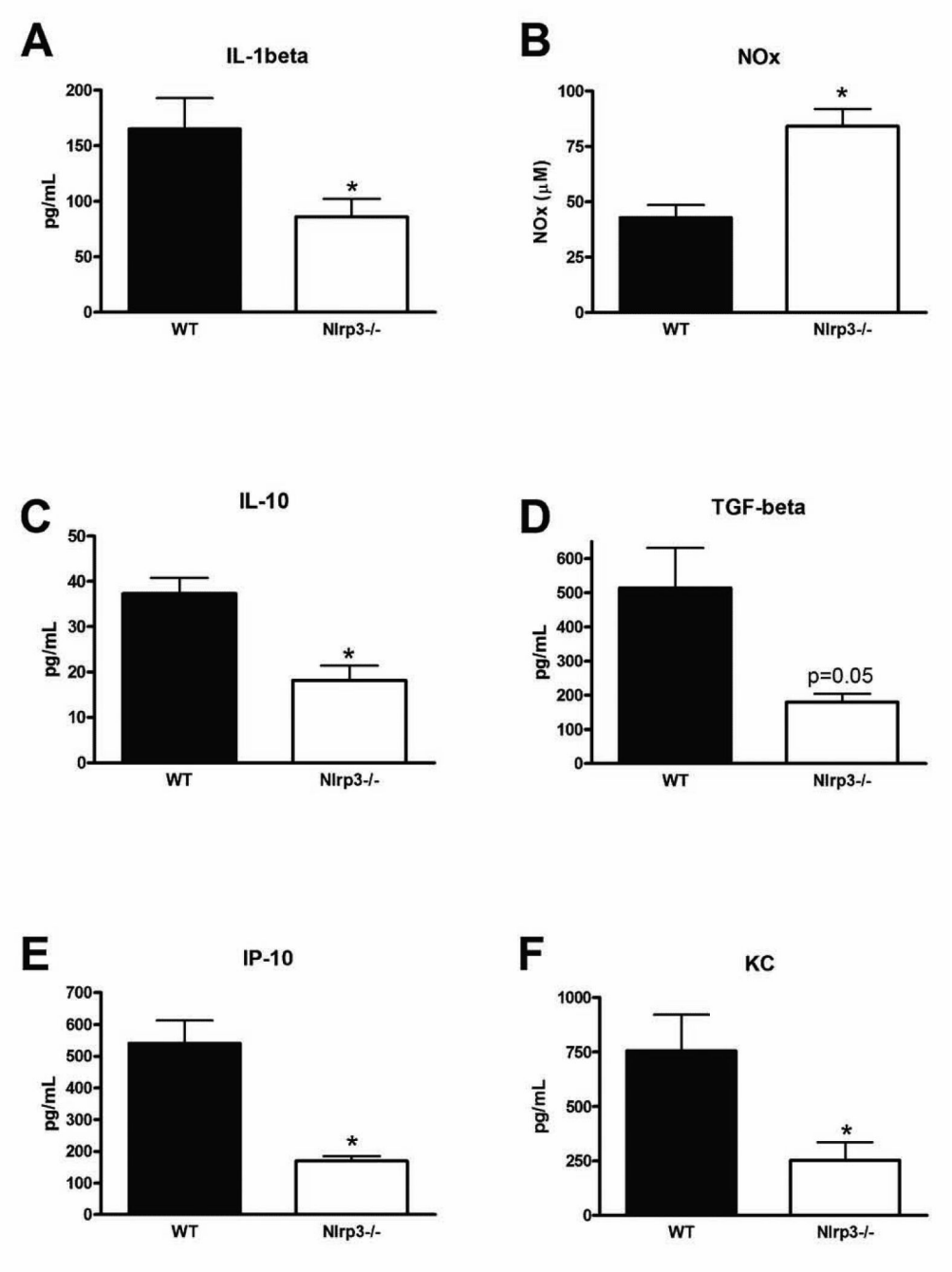

Figure 3.

Cytokine, chemokine and NOx levels are altered in Nlrp3$^{-/-}$ mice exposed to a 7-day course of DSS colitis when compared to WT mice. N=3-8/group; * denotes $p<0.05$ compared to levels observed in WT mice.

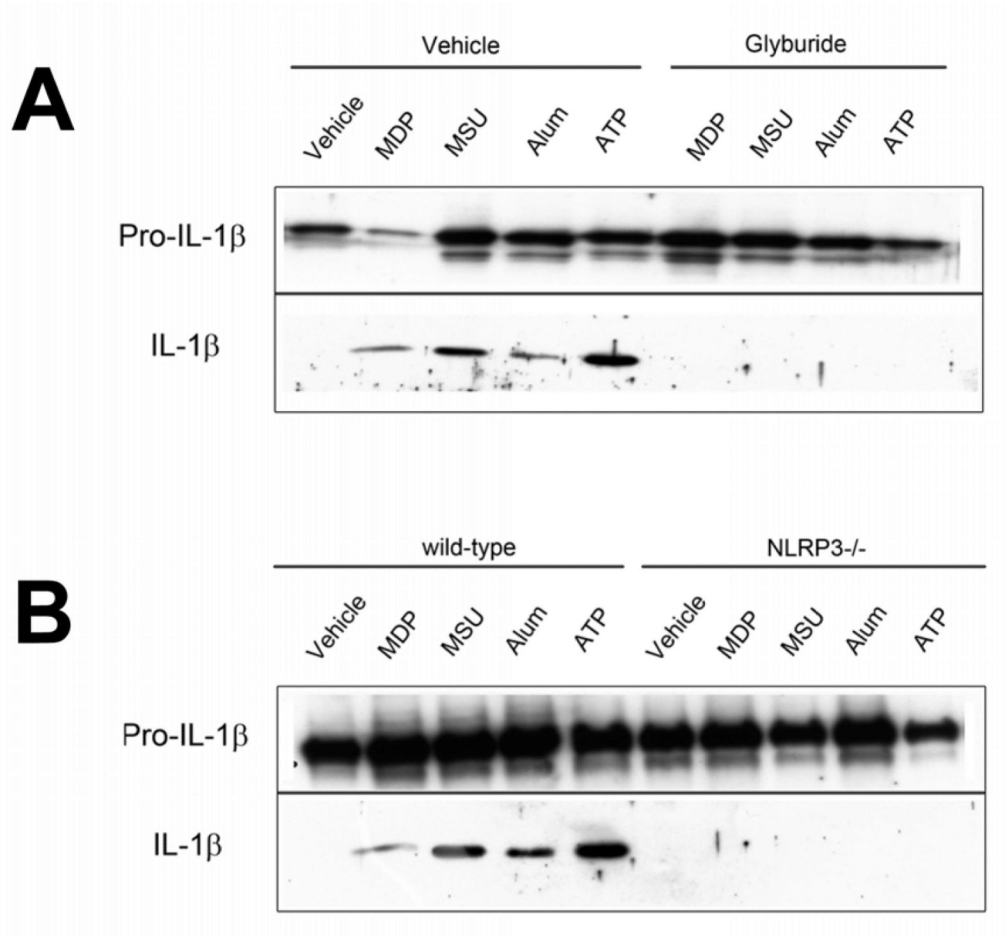

Figure 4.

Peritoneal macrophages isolated from Nlrp3-/- mice fail to respond to bacterial muramyl dipeptide (A) Macrophages pre-treated with ultra-pure lipopolysaccharide (LPS, 10ng/mL for 1h) exhibit IL-1β processing and release into culture media when exposed (6h) to muramyl dipeptide (MDP, 10μg/mL), monosodium urate crystals (MSU, 50μg/mL), aluminum adjuvant (Alum, 500μg/mL) and adenosine triphospate (ATP, 5mM). IL-1β processing is inhibited by glyburide (100μM), a selective inhibitor of the NLRP3-inflammasome, and absent in NLRP3-deficient macrophages (B). Western blot are representative of 4 separate experiments.

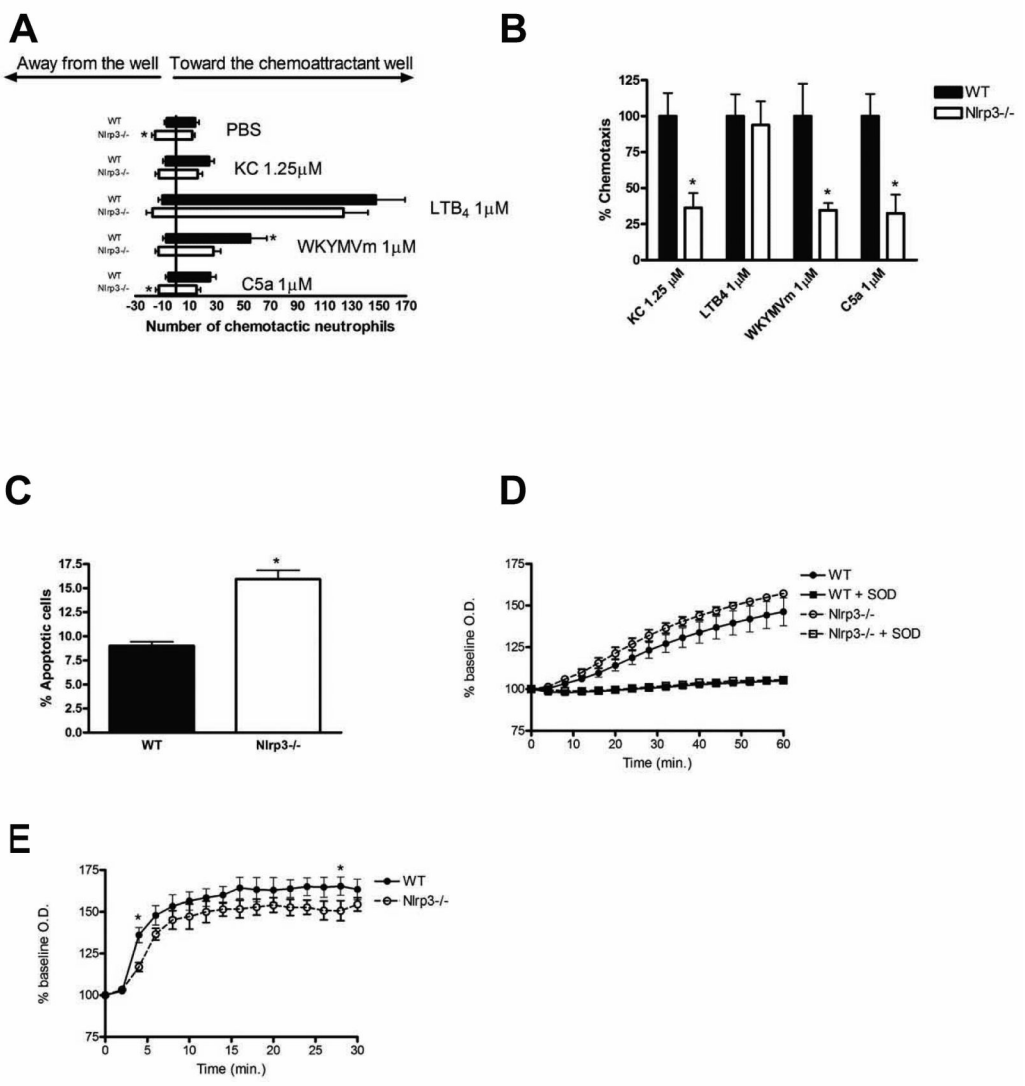

Figure 5.

Chemotaxis and spontaneous apoptosis are altered in BM-derived neutrophils isolated from Nlrp3$^{-/-}$ mice. (A) Overall neutrophil movement in response to PBS (vehicle control), KC (1.25 μM), leukotriene B4 (1 μM), WKTMVm (1 μM) and C5a (1 μM) as assessed with an under-agarose assay. (B) Neutrophil chemotaxis expressed as the number of cells that migrated towards the chemoattractant as a percentage of the total number of cells that moved in any direction. N=4; * denotes $p<0.05$ compared to WT cells. (C) Spontaneous apoptosis of BM-derived neutrophils after 12h in culture as assessed by flow cytometry. N=4; * denotes $p<0.05$ compared to WT cells. (D-E) Assessment of PMA(8 μM; D)- and fMLP(8 mM; E)-induced superoxide production in BM-derived neutrophils isolated from WT and Nlrp3$^{-/-}$ mice. N=4, * denotes $p<0.05$ compared to WT cells. Addition of superoxide dismutase (SOD, 1500 U) was employed as a control to quench superoxide accumulation (D).

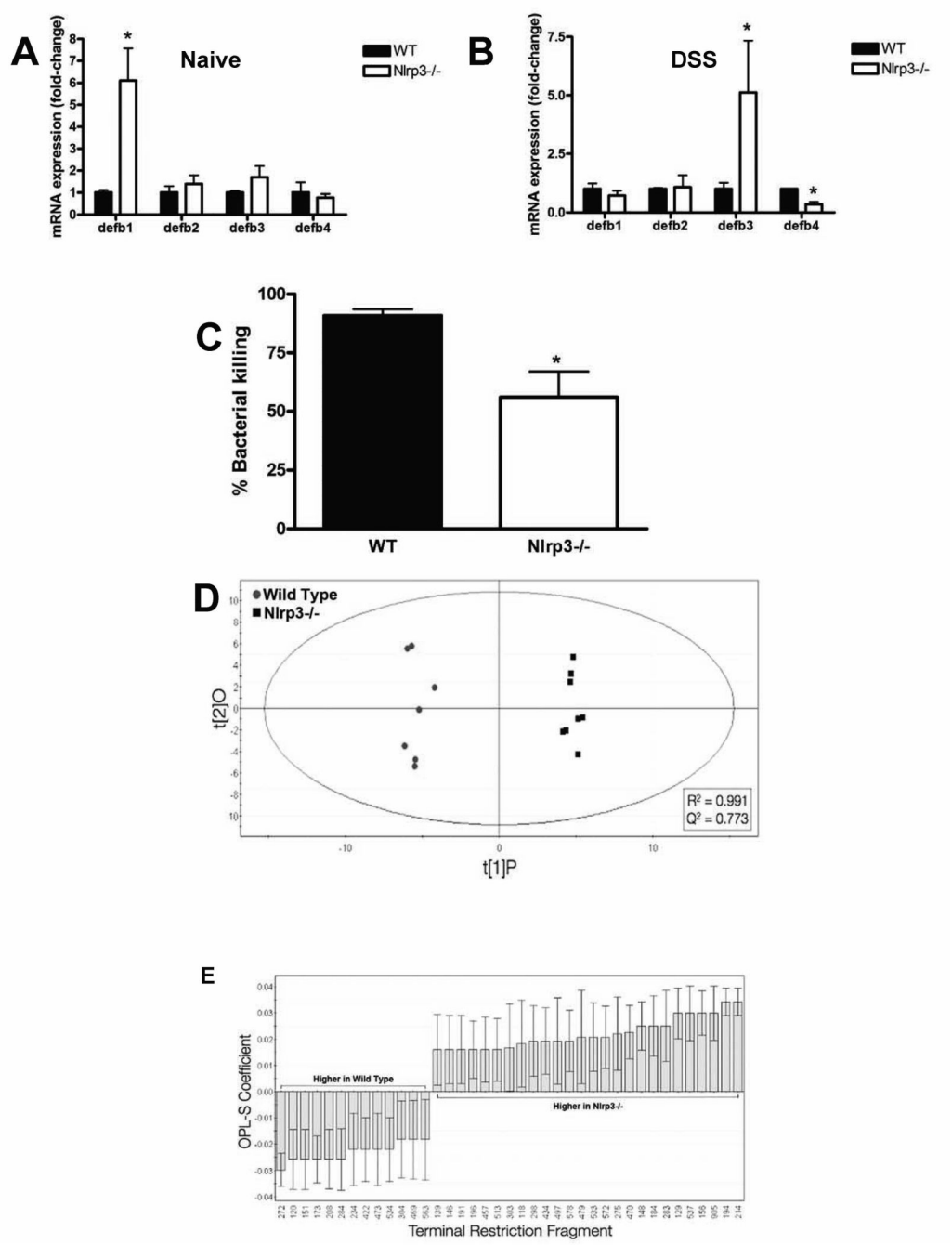

Figure 6.

Nlrp3$^{-/-}$ mice display altered expression of β-defensin transcripts and exhibit a unique intestinal microbiota. (A) qPCR assessment of β-defensin transcripts in naïve WT and Nlrp3$^{-/-}$ mice expressed as a fold-change. (B) qPCR assessment of β-defensin transcripts in DSS-treated WT and Nlrp3$^{-/-}$ mice expressed as a fold-change (7-day course of 2.5% DSS). *defb1*–mouse β-defensin 1; *defb2*–mouse β-defensin 2; *defb3*–mouse β-defensin 3; *defb4*–mouse β-defensin 4. * denotes $p<0.05$ compared to naïve WT mice; N=5/group. (C) The antimicrobial capacity of crypt secretions derived from WT and Nlrp3$^{-/-}$ mice. Overnight colony growth in secretion-treated *E. coli* cultures was compared to untreated cultures and expressed as percent reduction in colony numbers, termed percent killing. *

denotes $p<0.05$ compared to WT mice; N=3. (D) Supervised OPL-S discriminant analysis of TRFLP binary data shows that naïve Nlrp3$^{-/-}$ mice display a unique microbiota when compared to WT littermates. (E) Several unique TRFs were found to significantly distinguish the two groups. N=7/group for TRFLP analysis.

Table 1

Higher in Wild Type

TRF Size (bp)	Phylum	Class	Order	Family	Genus
272	Firmicutes	Clostridia	Clostridiales	Ruminococcaceae	Faecalibacterium
120	Proteobacteria	Betaproteobacteria	Rhodocyclales	Rhodocyclaceae	Rhodocyclaceae
208	Firmicutes	Clostridia	Clostridiales	Lachnospiraceae	Lachnospiraceae
534	Firmicutes	Clostridia	Clostridiales	Ruminococcaceae	Ruminococcaceae
563	Firmicutes	Bacili	Lactobacillales	Streptococcaceae	Streptococcus
139	Firmicutes	Erysipelotrichi	Erysipelotrichales	Erysipelotrichaceae	Erysipelotrichaceae

Higher in Nlrp3-/-

TRF Size (bp)	Phylum	Class	Order	Family	Genus
194	Firmicutes	Clostridia	Clostridiales	Ruminococcaceae	Ruminococcaceae
156	Firmicutes	Clostridia	Clostridiales	Lachnospiraceae	Lachnospiraceae
129	Actinobacteria	Actinobacteria	Coriobacteriales	Coriobacteriaceae	Collinsella
184	Firmicutes	Clostridia	Clostridiales	Ruminococcaceae	Subdoligranulum
275	Actinobacteria	Actinobacteria	Actinomycetales	Mycobacteriaceae	Mycobacterium
572	Firmicutes	Bacili	Lactobacillales	Lactobacillaceae	Lactobacillus
578	Firmicutes	Bacili	Clostridiales	Clostridiaceae	Clostridium
497	Proteobacteria	Gammaproteobacteria	Enterobacteriales	Enterobacteriaceae	Citrobacter/Proteus/ Shigella
434	Proteobacteria	Betaproteobacteria	Burkholderiales	Burkholderiaceae	Ralstonia
118	Lentisphaerae	Lentisphaerae	Unclassified Lentisphaerae	-	-